Aging-declined RNA exportation impairs hematopoietic stem cells by inducing R-loop

Ruiqing Chen,[1,2*] Qiongye Dong,[3*] Lihong Zhou,[1*] Hanqing He,[4] Yingxue Du,[5] Qianwen Sun,[5] Toshio Suda,[1] Tao Cheng[1] and Jianwei Wang[1,2,6]

[1]State Key Laboratory of Experimental Hematology, National Clinical Research Center for Blood Diseases, Haihe Laboratory of Cell Ecosystem, Institute of Hematology and Blood Diseases Hospital, Chinese Academy of Medical Sciences and Peking Union Medical College, Tianjin; [2]School of Pharmaceutical Sciences, Tsinghua University, Beijing; [3]Institute of Precision Medicine, Peking University Shenzhen Hospital, Shenzhen; [4]School of Biomedical Sciences, Hunan University, Changsha; [5]Center for Plant Biology and Tsinghua-Peking Joint Center for Life Sciences, School of Life Sciences, Tsinghua University, Beijing and [6]International Center for Aging and Cancer, Hainan Academy of Medical Sciences, Hainan Medical University, Haikou, China

**RC, QD and LZ contributed equally as first authors.*

Correspondence: T. Cheng
chengtao@ihcams.ac.cn

J. Wang
wangjianwei@ihcams.ac.cn

Received: March 6, 2025.
Accepted: June 26, 2025.
Early view: July 3, 2025.

https://doi.org/10.3324/haematol.2025.287765

Abstract

Aging-related accumulation of DNA damage adversely affects hematopoietic stem cell (HSC). However, the mechanisms underlying this accumulation and strategies for its elimination to rejuvenate aged HSC remain largely obscure. This study uncovers a notable surge in R-Loop presence within aged HSC, notably co-localized with γH2AX and replication protein A (RPA), and correlated with RNA residency in the nucleus. Targeted induction of R-Loop impairs the function of HSC. Mechanistically, RNA exportation is compromised in aged HSC due to a decline in Alyref, the primary constituent of the transcription-export complex (TREX). Specifically, *Alyref* dysfunction results in RNA retention within the nucleus, mimicking the functional characteristics of aged HSC. The nuclear accumulation of RNA leads to the formation of RNA:DNA hybrids, known as R-Loop structures, consequently inducing replication stress and DNA damage. Introducing a quantitative boost of *Alyref* in aged HSC notably reinstates RNA transportation, diminishes R-Loop formation and replication stress, and ultimately enhances the performance of aged HSC. Taken together, our research demonstrates the initial revelation that aging-triggered replication stress stems from abnormal RNA transportation-propelled R-Loop configurations, hinting at the potential of quantitatively modulating RNA transportation to mitigate the physiological drawbacks of aging on HSC.

Introduction

The diminished regenerative capability of tissue-specific stem cells due to aging contributes significantly to disruptions in tissue equilibrium during the aging process.[1-3] Hematopoietic stem cells (HSC) are responsible for life-span cell production,[4] and experience a decline in reconstitution capacity with aging.[5] Moreover, aged HSC display a bias towards myeloid lineage differentiation,[6-8] posing a risk factor for various hematopoietic malignancies.[9] Therefore, elucidating the molecular mechanisms underlying HSC aging and devising strategies to anti-aging intervention for aged HSC function will unquestionably benefit the elderly and individuals afflicted by hematopoietic system degenerative changes.

We and others have previously shown that DNA damage accumulation, characterized by γH2AX, has been considered one of the driving forces of HSC aging.[10-15] Faithful DNA replication is pivotal for the maintenance of genome stability. Any molecular event interfering with DNA replication, collectively named replication stress, makes DNA molecules more vulnerable to damage, mutations, or genomic instability.[16-18] A previous study has shown that replication stress is a potent driver of functional decline in aged HSC.[10] While, the critical cellular signaling leading to replication stress in aged HSC has not been clearly elucidated. In this study, we observed that R-Loop, a three-stranded nucleic acid structure consisting of a DNA:RNA hybrid and a displaced strand of DNA, which is generated during DNA transcription,[19,20] accumulated in aged HSC, which impairs HSC by inducing replication stress and DNA damage. Mechanistically, the retention of RNA in nucleus of aged HSC,

induced by the aging-declined RNA exportation, results in the increase of R-Loop.

Methods

Mice

Alyref$^{flox/flox}$ mice were generated in Cyagen Biosciences Inc. (Guangzhou, China). Alyref$^{flox/flox}$ mice (C57BL/6N) were generated by inserting loxP sites spanning the third exon of *Alyref* via homologous recombination. To achieve hematopoietic-specifically knockout mice, Alyref$^{flox/flox}$ were crossed to Mx1-Cre mice. To induce Cre expression in Mx1-Cre^{+}; Alyref$^{flox/flox}$ mice were intraperitoneally injected with Poly I:C (25 mg/kg) every other day for 14 days. All genotyping primers are listed in *Online Supplementary Table S1*.

The recipients used in the competitive transplantation assays were CD45.1/2 that were the first generation of C57BL/6 (CD45.2) and B6.SJL (CD45.1) mice. All mice were housed in specific-pathogen-free facilities, and all procedures were approved by the Institutional Animal Care and Use Committee (IACUC) of Tsinghua University.

RNA fluorescent *in situ* hybridization

RNA fluorescent *in situ* hybridization (FISH) was conducted using a Ribo fluorescence *in situ* hybridization kit (RiboBio, C10910) in accordance with the manufacturer's directions. For the R-Loop and mRNA co-localization assay, cells were performed for RNA FISH after cells incubated by anti-DNA-RNA hybrid, clone S9.6 and secondary antibodies.

Cytoplasmic and nuclear RNA fractionation and sequencing

The cytoplasmic and nuclear fractions derived from CD34^{-} LSK cells were used to generate cDNA libraries, which were sequenced with 150-bp paired-end reads on an Illumina instrument by Novogene.

R-Loop peak calling

Strand-specific peaks were called by MACS3 (v3 3.0.0b1) with R-Loop and input samples. Peaks with q values less than 0.01 and enrichment score more than 10, and located outside the blacklisted region were defined as R-Loop peaks. We annotate peaks with genomic regions by R package ChIP seeker.

Single-strand DRIP-sequencing and single-strand DRIP-quantitative polymerase chain reaction

Single-strand DRIP-sequencing (ssDRIP-seq) library construction was performed according to published procedures.[21] Freshly isolated CD34^{-} LSK cells were lysed in DNA lysis buffer and incubated at 37°C. Genomic DNA was fragmented using restriction enzymes and subjected to DRIP with the S9.6 antibody. DRIP DNA was validated by quantitative polymerase chain reaction (qPCR) or sonicated for ssDRIP-seq library construction, followed by sequencing on an Illumina NovaSeq system.

dCas9 coupled RNaseH1 D209N-mediated site-specific R-Loop

dCas9 coupled RNaseH1 D209N-mediated site-specific R-Loop was performed as previously published.[22] In brief, dCas9 infused with RNaseH1 D209N was co-expressed with gRNA targeting the selected R-Loop sites in NIH-3T3 cells. mCherry^{+} cells were purified for ssDRIP-qPCR and immunofluorescence staining. The gRNA and qPCR primers are listed in *Online Supplementary Table S6*.

RNA sequencing

In brief, 50 HSC were sorted directly into lysis buffer. Then the RNA sequencing (RNA-seq) library was prepared using the method of Smart-seq2. After the library construction, the insertion size was assessed by Agilent Bioanalyzer 4200 system (Agilent Technologies), and the accurate insertion size was quantified by Taqman fluorescence probe of AB Step One Plus Real-Time PCR system. Clustering of the index-coded samples was performed using HiSeq PE Cluster Kit v4-cBot-HS (Illumina) following the manufacturer's instructions. The libraries were sequenced by an Illumina Hiseq platform with 150-bp paired-end. The transcriptome sequencing was performed by ANNOROAD Gene Technology Company.

Statistical analysis

Data are shown as mean ± standard deviation (SD). Student's *t* test (two-tailed unpaired) were used for comparisons (GraphPad Prism v.7.0). NS: not significant; **P*<0.05; ***P*<0.01; ****P*<0.001; *****P*<0.0001. All experiments were repeated two or three times.

Results

R-Loop is increased in aged hematopoietic stem cells

We conducted immunofluoresence for R-Loop using the S9.6 antibody,[23] and observed accumulated R-Loop foci in aged HSC (Figure 1A-D), with RNase H, but not RNase III, serving as a positive control to dissolve R-Loops.[24,25]

We then profiled genome-wide R-Loop at single-nucleotide resolution in young and aged HSC to systemically examine the correlation of R-Loops with aging by conducting ssDRIP-seq according to a recently developed method[21] (*Online Supplementary Figure S1A*). As expected, R-Loops correlate with high G/C skewing in both young and aged HSC (Figure 1E), indicating accurate mapping of R-Loops by ssDRIP-seq data. We then examined the global distribution of age-associated changes in R-Loops across the mouse genome. The results show that most R-Loops are located in the intergenic region (~50%) and gene body region (~40%), which includes the 5'UTR, 3'UTR, exons, and introns, with no significant differences observed between

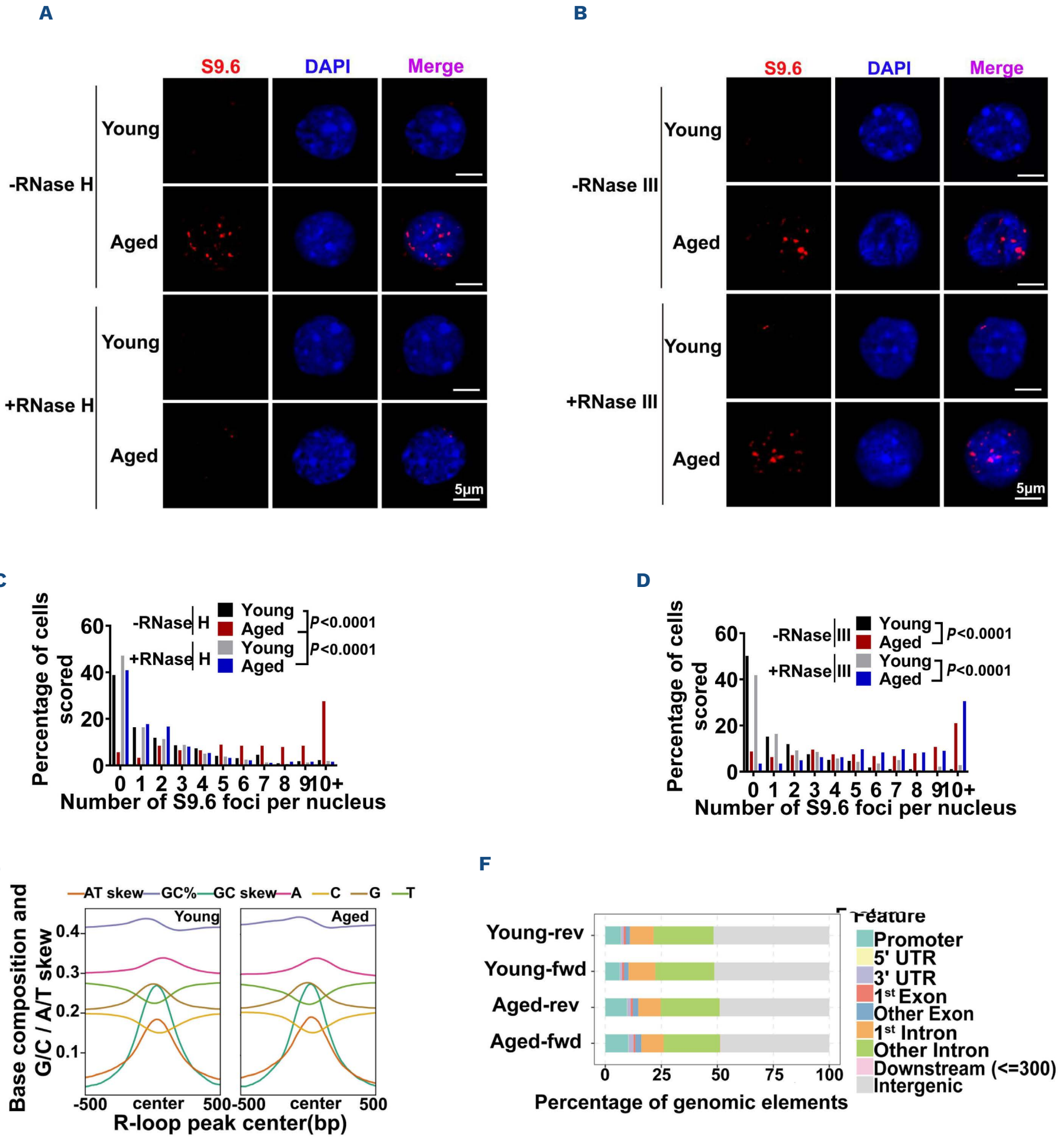

Figure 1. R-Loop is increased in aged hematopoietic stem cells. (A) Representative images depicting immunofluorescence staining of S9.6 in both young and aged hematopoietic stem cells (HSC). Freshly isolated HSC (CD34$^-$ Flt3$^-$ LSK) from young (2 months) and aged (24-30 months) mice were subjected to immunofluorescence staining. The cells were either left untreated (-RNase H) or were instead treated with RNase H (+RNase H). The panels are shown at the same exposure. The cell nuclei were stained with DAPI. (B) Representative images depicting immunofluorescence staining of S9.6 in both young and aged HSC. Freshly isolated HSC from young (2 months) and aged (24-30 months) mice were subjected to immunofluorescence staining. The cells were either left untreated (-RNase III) or were instead treated with RNase III (+RNase III). The panels are shown at the same exposure. The cell nuclei were stained with DAPI. (C-D) S9.6 foci distribution in both young and aged HSC treated with RNase H (C) or RNase III (D). (E) Metaplot showing G/C skews, A/T skews, G/C contents and base compositions in 500 bp upstream and downstream regions of R-Loop peak summits in young and aged HSC. (F) Barplot showing the genomic distribution of R-Loop strand-specific peaks (forward and reverse strand separately) in both young and aged HSC.

young and aged HSC (Figure 1F). However, 6.6% of R-Loop peaks are located in the promoter region of young HSC, and this significantly increases to 10% with aging (Fisher's exact test, odd ratio =1.5; *P*=1.97e-10) (Figure 1F). To further characterize the increase of R-Loops with aging, we performed a genome browser inspection and observed a significant increase in R-Loop signals from 2 kb upstream of the TSS to downstream of the TES in aged HSC (*Online Supplementary Figure S1B*). Additionally, we noted increased R-Loop coverage in aged HSC (*Online Supplementary Figure S1C*), which aligns with previous reports.[26] We quantified the peak width in aged and young samples. Consistent with these observations, the results show that the width of R-Loop peaks exhibit significant increase in aged HSC (*Online Supplementary Figure S1D*). To delve deeper into the molecular characteristics influenced by aging-associated increases in R-Loops, we conducted gene set enrichment analysis (GSEA) of genes ranked based on their differential R-Loop signals in the gene body region between aged and young HSC. The results indicate that the augmented presence of R-Loops is enriched with genes associated with cell aging and myeloid functions, which is a classical feature of aged HSC (*Online Supplementary Figure S1E*; *Online Supplementary Table S7*).

Accumulated R-Loop induces DNA damage and impairs the function of hematopoietic stem cells

Previous studies have demonstrated that aged HSC accumulate DNA damage, as evidenced by increased γH2AX foci.[11] To investigate this further, we conducted whole-genome sequencing of young and aged HSPC to identify such damage between them. Surprisingly, we observed no significant increase in insertions and deletions (InDels) in aged HSPC, suggesting that physiological DNA breaks are not elevated with aging (Figure 2A). Subsequently, we performed immunofluorescence staining for γH2AX and R-Loops in aged HSC. The results revealed co-localization between them (Figure 2B). Since γH2AX is also indicative of replication stress,[10] we further investigated immunofluorescence staining for RPA, a marker of replication stress.[10,17,27,28] Remarkably, R-Loops co-localized with RPA foci in aged HSC (*Online Supplementary Figure S2A*), indicating an association between R-Loops and replication stress during aging.

To further explore the causal relationship between R-Loops and DNA damage, we focused on Nfe2l2, which modulates the migration and retention of HSC[29] and is enriched with R-Loop in aged HSC (Figure 2C). Upon introducing an R-Loop in the intron of *Nfe2l2* (*Online Supplementary Figure S2B;* Figure 2D, refer to the Methods section for details), we observed the accumulation of RPA and γH2AX foci (Figure 2E, F), suggesting that the elevation of R-Loops indeed triggers DNA damage in HSC.

To further investigate the causation between R-Loop and the functional decline of HSC, we generated two efficient small hairpin (sh)RNA against *RNaseH1* and *RNaseH2A* (*Online Supplementary Figure S2C*), the key enzymes responsible for dissolving R-Loops.[30-32] By conducting a competitive transplantation assay, we observed that knockdown of these enzymes impairs the reconstitution capacity of HSC and promotes a myeloid differentiation bias (*Online Supplementary Figure S2D, E*), which are key features of aged HSC. Bone marrow (BM) analysis exhibited compromised reconstitution capacity and a reduction of HSC upon knockdown of these enzymes (*Online Supplementary Figure S2F, G*). Moreover, we purified GFP^+ hematopoietic stem and progenitor cells from the recipients at the end of the third month and examined the level of R-Loop. The results show that the level of R-Loop is significantly increased in cells carrying shRNaseH1 and shRNaseH2A (*Online Supplementary Figure S2H, I*). It is notable that these cells exhibit significant increased γH2AX foci (*Online Supplementary Figure S2J, K*).

In brief, the above data suggest that the accumulation of R-Loops co-localizes with DNA damage signal and results in the functional decline of HSC.

Aging-increased R-Loop correlates with the lingering RNA in the nucleus of hematopoietic stem cells

Given that the R-Loop is a microstructure of chromosomes composed of DNA:RNA strands, we then hypothesize whether the increase in R-Loops correlates with the retention of RNA in the nucleus of aged HSC. To explore this hypothesis, we categorized the genes into four groups based on the fold change of R-Loop signals between aged and young HSC: category-1 having the greatest loss of R-Loops and category-4 with the greatest gain of R-Loops. The results reveal that genes showing increased R-Loop formation display a higher ratio of nuclear to cytoplasmic RNA with aging (Figure 3A). This suggests that the accumulation of RNA in the nucleus of aged HSC might contribute to the formation of R-Loops.

To corroborate this observation, we focused on two genes: *Nfe2l2* and *Adgrg1*, which play crucial role in regulating HSC.[29,33] Our observations indicate that the mRNA of *Nfe2l2* and *Adgrg1* accumulate in the nucleus of aged HSC (Figure 3B, C). Moreover, the R-Loop signal across the *Nfe2l2* and *Adgrg1* loci increases with aging (Figures 2C and 3D). RNA FISH and immunofluorescence staining reveal the co-localization of their RNA and the accumulated R-Loops within them (Figure 3E).

In summary, these findings suggest that R-Loops are heightened in aged HSC and are associated with the accumulation of RNA in nucleus during aging.

RNA exportation is impaired in aged hematopoietic stem cells

We then conducted an RNA FISH assay to assess the bulk poly(A)$^+$RNA distribution between the nucleus and cytoplasm of both young and aged HSC, aiming to scrutinize RNA distribution patterns associated with aging. Our findings indicate a notable accumulation of mRNA within

A

Samples	InDel number
Young-1	182933
Young-2	176499
Aged-1	165579
Aged-2	161090

B

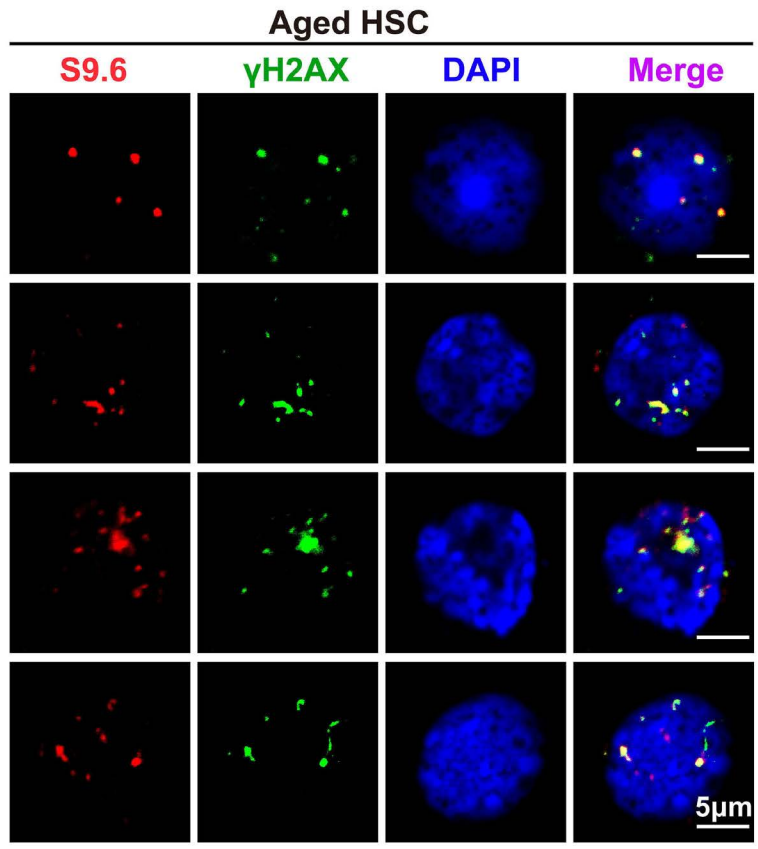

C

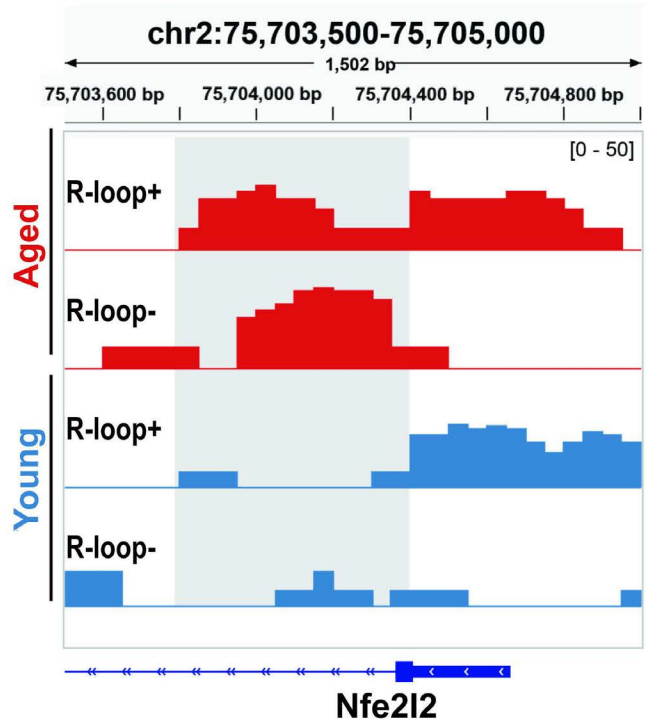

D

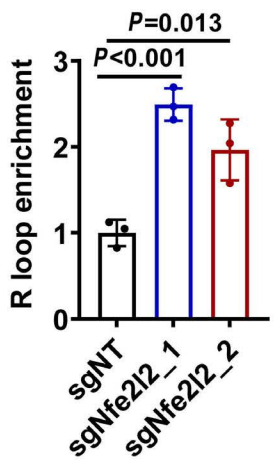

E

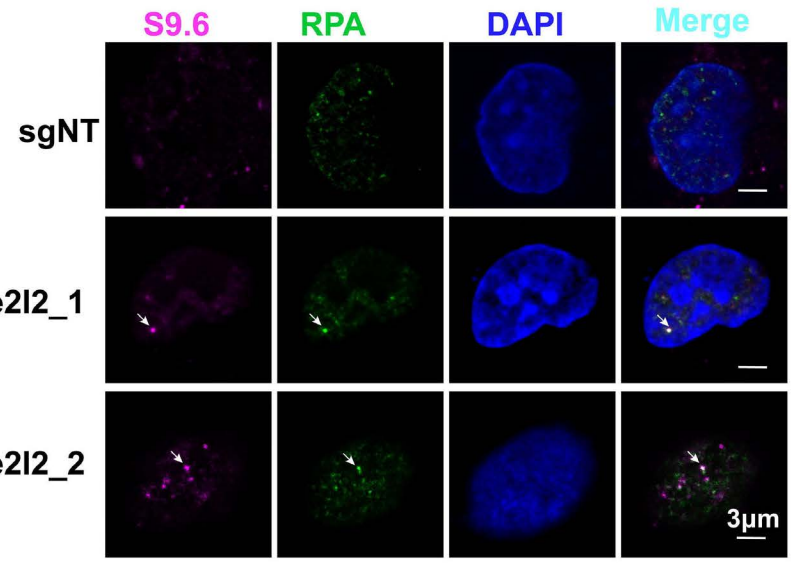

F

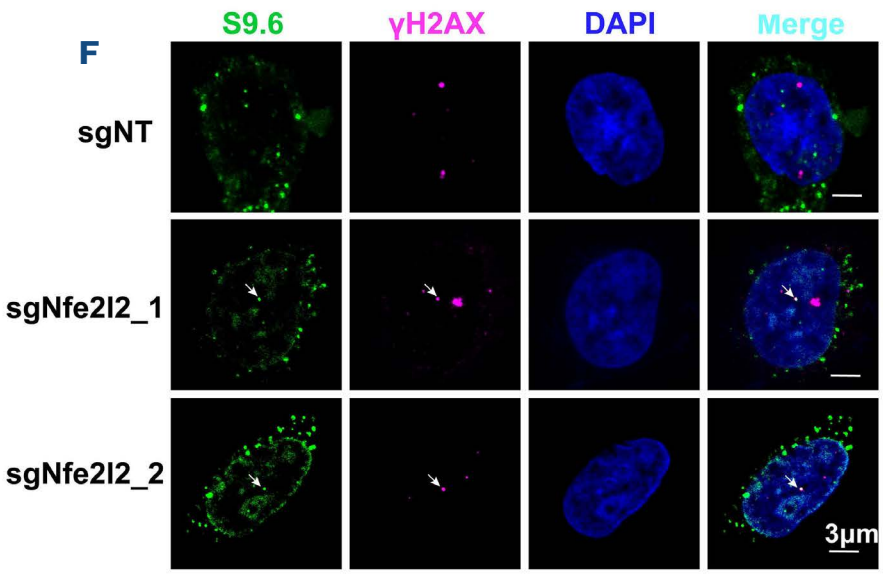

Figure 2. Accumulated R-Loop induces DNA damage and impairs the function of hematopoietic stem cells. (A) The absolute number of insertions and deletions (InDels) in young (2 months) and aged (24-30 months) hematopoietic stem and progenitor cells (HSPC). Freshly isolated LSK cells from young and aged mice were subjected to whole-genome sequencing. (B) Representative fluorescence images depicting the co-localization of the R-Loop with γH2AX in aged hematopoietic stem cells (HSC). (C) Representative tracks showing aged HSC-specific R-Loop peaks (red, aged HSC; blue, young HSC) in the region comprising *Nfe2l2*. (D) single strand DRIP-quantitative polymerase chain reaction (ssDRIP-qPCR) monitoring of the R-Loop levels at specific regions. Data are presented as mean ± standard deviation. (E, F) Representative fluorescence images depicting the co-localization of the R-Loop with RPA (E) and γH2AX (F) in NIH-3T3 cells.

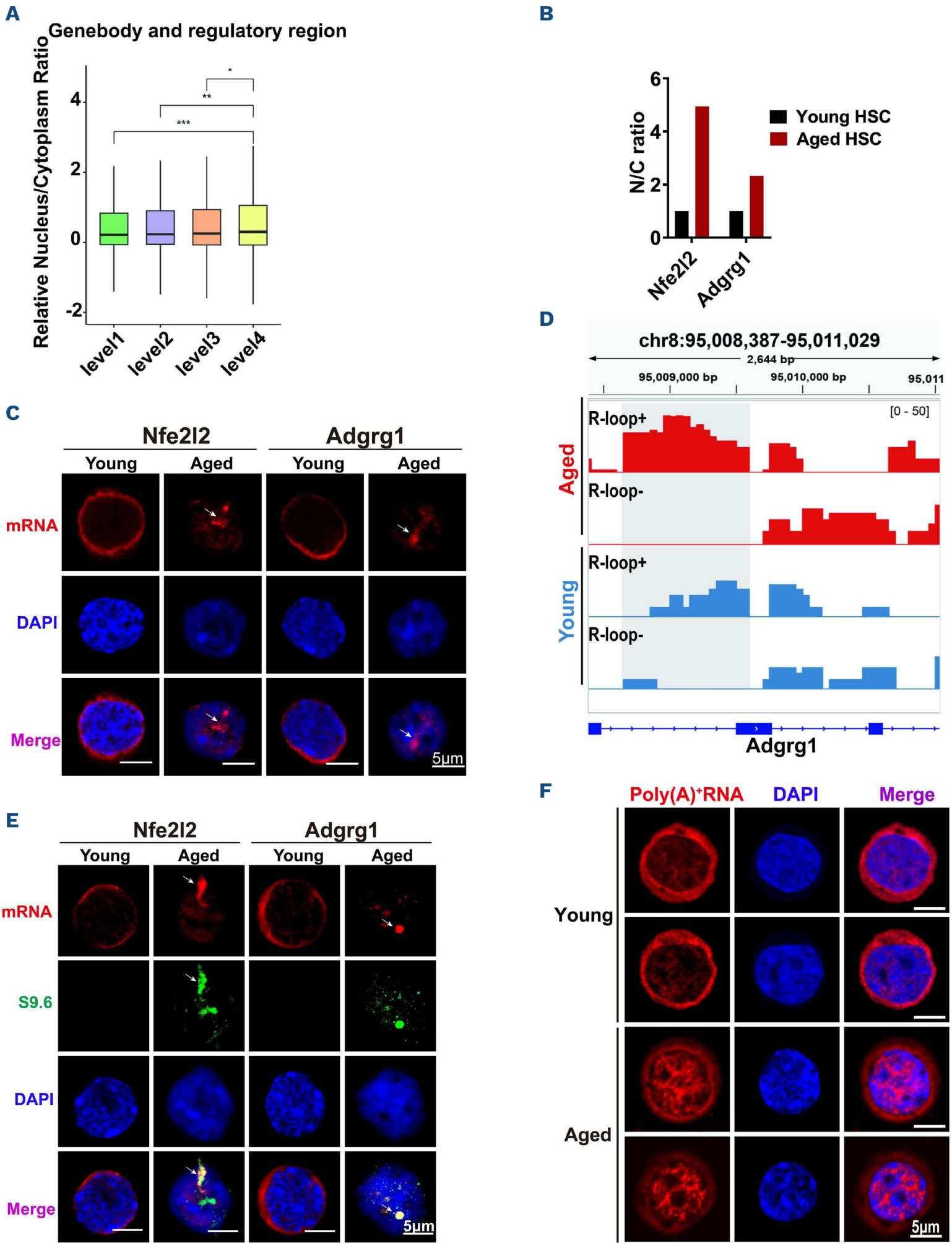

Figure 3. Aging-increased R-Loop correlates with the lingering RNA in the nucleus of hematopoietic stem cells. (A) Boxplot of the relative nucleus/cytoplasm ratio in four groups of genes with different R-Loop signal changes that occurred during aging. DESeq2 was performed to measure the difference in single strand (ss)DRIP reads in the gene body and its regulatory region in both young and aged hematopoietic stem cells (HSC). The genes were divided into 4 groups according to the quantiles of the DESeq2 test statistic. Genes belonging to level 1 have the highest R-Loop loss, while genes in level 4 have the highest R-Loop gain. The Y-axis indicates the nucleus/cytoplasm ratio of aged samples divided by the same ratio in young samples (one sided

Continued on following page.

Wilcoxon signed rank test). (B) Histograms depicting the nuclear and cytoplasmic mRNA ratio of *Nfe2l2* and *Adgrg1* in both young and aged HSC. The data were obtained from nuclear and cytoplasmic RNA sequencing (RNA-seq). (C) Representative images depicting the *Nfe2l2* and *Adgrg1* mRNA in aged HSC. Freshly isolated HSC from young (2-month-old) and aged (24-27-month-old) mice were subjected to the assay. The panels are shown at the same exposure. The cell nuclei were stained with DAPI. (D) Representative tracks showing aged HSC-specific R-Loop peaks (red, aged HSC; blue, young HSC) in the region comprising *Adgrg1*. (E) Representative images depicting the co-localization of the R-Loop with *Nfe2l2* and *Adgrg1* mRNA in aged HSC. Freshly isolated HSC from young (2-month-old) and aged (24-27-month-old) mice were subjected to the co-localization assay. The panels are shown at the same exposure. The cell nuclei were stained with DAPI. (F) Representative images showing the distribution of Poly(A)$^+$RNA in young and aged HSC. These images were obtained by subjecting freshly isolated HSC (CD34$^-$ Flt3$^-$ LSK) from young (2 months) and aged (24-30 months) mice to RNA fluorescence *in situ* hybridization (FISH) using a Cy3-labeled oligo(dT)$_{50}$ probe to visualize poly(A)$^+$RNA. Nuclei were stained with DAPI. The panels are shown at the same exposure for accurate comparison.

the nucleus of aged HSC compared to their younger counterparts (Figure 3F; *Online Supplementary Figure S3A*). To corroborate this observation, we analyzed the profiles of nuclear and cytoplasmic RNA from both young and aged HSC. The results unequivocally demonstrate a significant increase in mRNA accumulation within the nucleus of aged HSC (*Online Supplementary Figure S3B*).

To unravel the molecular mechanisms underlying this phenomenon, we initiated an integrative analysis of five previously published datasets (RNA-seq data of young and aged HSC).[34-38] Our examination revealed a significant enrichment of Gene Ontologies related to RNA localization with aging (*Online Supplementary Figure S3C*). Delving deeper, we found a notable impairment in the RNA transportation pathway within aged HSC (*Online Supplementary Figure S3D*), with *Alyref* emerging as the most significantly downregulated gene (*Online Supplementary Figure S3E*). Subsequently, we embarked on validating the alteration of *Alyref* expression between young and aged HSC, confirming a marked decrease in *Alyref* at both the mRNA and protein levels with aging (*Online Supplementary Figure S3F, G*).

Targeted dysfunction of *Alyref* induces R-Loop and disrupts hematopoietic homeostasis

To probe the functional implications of *Alyref* in HSC aging, we generated Alyref$^{flox/flox}$ mice (*Online Supplementary Figure S4A*), and bred them with Mx1-Cre mice to produce Mx1-Cre; Alyref$^{flox/flox}$ and Mx1-Cre; Alyref$^{flox/+}$ offspring. Upon poly I:C treatment for 14 days, *Alyref* is uniformly and heterozygously deleted in hematopoietic cells yielding Alyref$^{-/-}$ and Alyref$^{+/-}$ mice, respectively (*Online Supplementary Figure S4B, C*). We observed increased and co-localized signals among R-Loops, γH2AX and RPA in Alyref$^{-/-}$ and Alyref$^{+/-}$ HSC (Figure 4A, B; *Online Supplementary Figure S4D, E*). Additionally, replication fork assays exhibited increased replication stress in Alyref$^{+/-}$ (Figure 4C), Alyref$^{-/-}$ HSC (Figure 4D) and aged HSC (Figure 4E). Collectively, these data indicate that dysfunction of *Alyref* lead to an increase in R-Loops, DNA damage and replication stress in HSC.

We then sought out to examine the hematopoietic phenotype of Alyref$^{+/-}$ and Alyref$^{-/-}$ mice. Complete blood count assay revealed a notable decrease in white blood cell (WBC), neutrophil (NEUT), lymphocyte (LYM), basophilic granulocyte (BAS) and platelet (PLT) counts in Alyref$^{-/-}$ mice, contrasting with Alyref$^{+/-}$ counterparts (Figure 4F). However, both strains exhibited a drop in red blood cell (RBC), hemoglobin (HGB) and hematocrit (HCT) levels (Figure 4F; *Online Supplementary Figure S4F*). The BM cellularity of Alyref$^{-/-}$ mice exhibited a significant decrease compared to their littermate controls (*Online Supplementary Figure S4G*). Subsequently, we delved into investigating the lineage composition in the peripheral blood (PB) and BM of both Alyref$^{+/-}$ and Alyref$^{-/-}$ mice, focusing on T cells, B cells, and myeloid cells. Our analysis unveiled a significant increase in T-lineage cells and a decrease in B and myeloid lineages in both PB and BM of Alyref$^{-/-}$ mice, contrasting with Alyref$^{+/-}$ mice (*Online Supplementary Figure S4H, I*). Moving forward, we scrutinized the hematopoietic stem and progenitor cells of these mice, encompassing common myeloid progenitor (CMP), granulocyte-macrophage progenitor (GMP), megakaryocyte-erythroid progenitor (MEP), common lymphoid progenitor (CLP), multipotent progenitor cell (MPP), short-term hematopoietic stem cell (ST-HSC) and long-term hematopoietic stem cell (LT-HSC). Strikingly, our findings demonstrated a dramatic decrease in all populations within Alyref$^{-/-}$ mice, while no such effect was observed in Alyref$^{+/-}$ mice (*Online Supplementary Figure S4J-L*). These findings suggest that short-term heterozygous deletion of *Alyref* does not significantly impact hematopoietic homeostasis. To further explore the long-term effects, we retained Alyref$^{+/-}$ mice for 10 months and observed an increase in RNA accumulation within the nucleus of HSC (*Online Supplementary Figure S4M, N*). Notably, complete blood count assay revealed evident decreases in WBC, LYM, HGB and HCT levels (*Online Supplementary Figure S4O*). Moreover, the BM cellularity of Alyref$^{+/-}$ mice displayed a mild decrease compared to their littermate controls (*Online Supplementary Figure S4P*). Further analysis of lineage composition unveiled a significant decrease in B lineage cells and a mild increase in myeloid lineage cells in the peripheral blood, but not bone marrow, of Alyref$^{+/-}$ mice (*Online Supplementary Figure S4Q, R*). Additionally, hematopoietic stem and progenitor cells (LSK), ST-HSC, GMP and CLP exhibited a significant decrease in Alyref$^{+/-}$ mice (*Online Supplementary Figure S4S, T*).

In summary, these data collectively indicate that Alyref

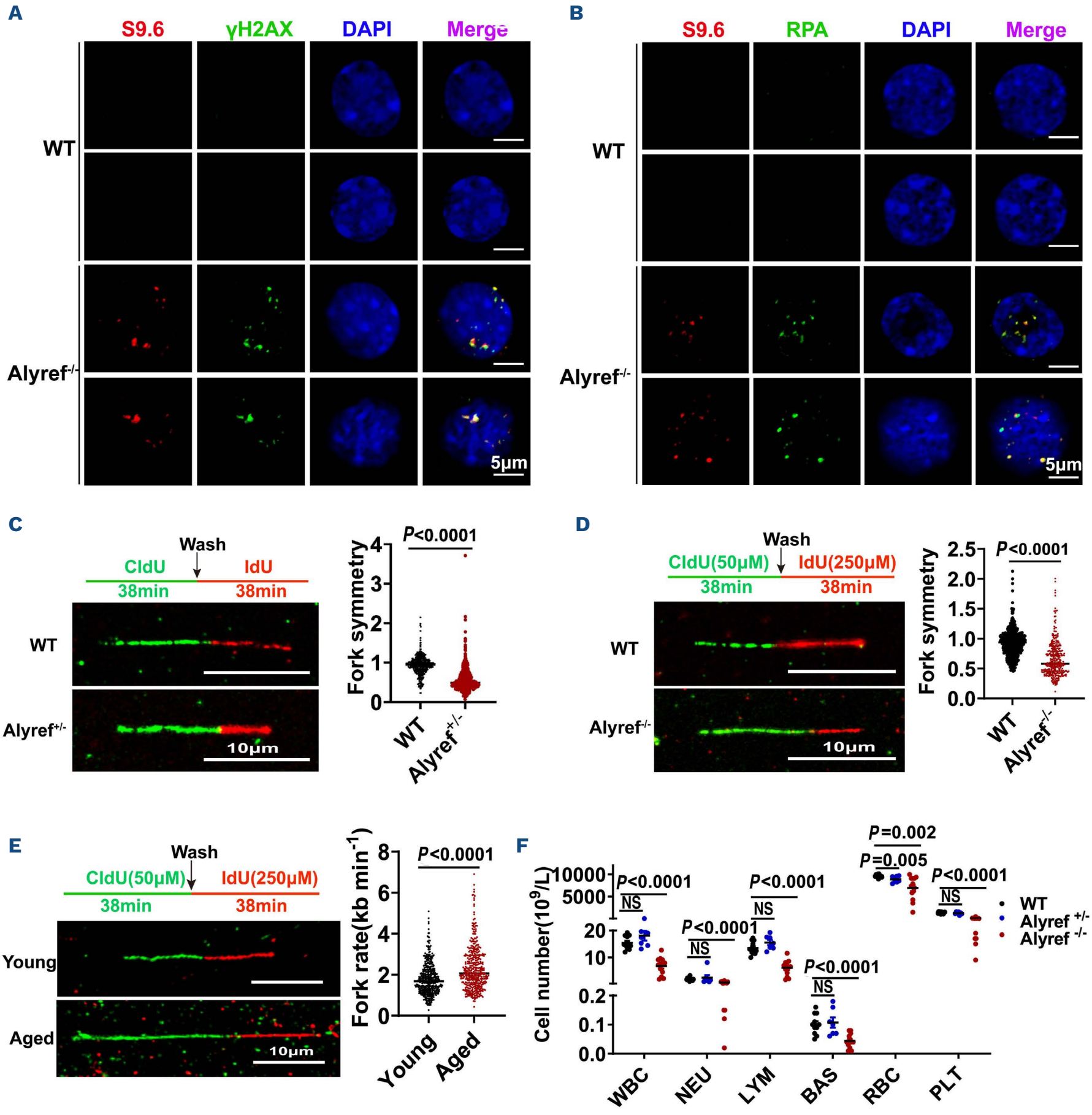

Figure 4. Targeted dysfunction of *Alyref* induces R-Loop and disrupts hematopoietic homeostasis. (A, B) Representative fluorescence images depicting the co-localization of the R-Loop with RPA (A) and γH2AX (B) in Alyref$^{-/-}$ hematopoietic stem cells (HSC). (C, left representative image) Representative images depicting the CldU/IdU-labeled DNA replication tracks in wild-type (WT) and Alyref$^{+/-}$ HSC (12 months). (C, right dot plot) Dot plots depicting the DNA replication fork symmetry in WT and Alyref$^{+/-}$ HSC. The dot plot of ldU to CldU track length ratios for individual replication forks. Data are represented as mean ± standard deviation (SD). A minimum of 493 molecules were analyzed in each group. (D, left representative image) Representative images depicting the CldU/IdU-labeled DNA replication tracks in WT and Alyref$^{-/-}$ HSC (2-4 months). (D, right dot plot) Dot plots depicting the DNA replication fork symmetry in WT and Alyref$^{-/-}$ HSC. The dot plot of ldU to CldU track length ratios for individual replication forks. Data are represented as mean ± SD. A minimum of 358 molecules were analyzed in each group. (E, left representative image) Representative images depicting the CldU/IdU-labeled DNA replication tracks in young (3 months) and aged HSC (24 months). (E, right dot plot) Dot plots depicting the DNA replication fork symmetry in young and aged HSC. The dot plot of ldU to CldU track length ratios for individual replication forks. Data are represented as mean ± SD. A minimum of 423 molecules were analyzed in each group. (F) The dot plot displays the counts of white blood cells (WBC), neutrophils (NEUT), lymphocytes (LYM), red blood cells (RBC), basophilic granulocytes (BAS) and platelets (PLT) in WT, Alyref$^{+/-}$ and Alyref$^{-/-}$ mice. The data are based on at least 7 mice per group and are presented as mean ± SD.

plays a crucial and dosage-dependent role in maintaining hematopoietic homeostasis.

Targeted dysfunction of *Alyref* impairs hematopoietic stem cells

Subsequently, we conducted a competitive transplantation assay to assess the reconstitution capacity of Alyref$^{+/-}$ and Alyref$^{-/-}$ HSC (*Online Supplementary Figure S4U*). The findings revealed compromised reconstitution capacity in both Alyref$^{+/-}$ and Alyref$^{-/-}$ HSC (*Online Supplementary Figure S4V, W*). Notably, the reconstitution capacity of Alyref$^{-/-}$ HSC was significantly lower than that of Alyref$^{+/-}$ HSC, suggesting a dosage-dependent effect of *Alyref* on HSC function. To further evaluate the self-renewal capacity of Alyref$^{+/-}$ and Alyref$^{-/-}$ HSC, we conducted a secondary transplantation assay using BM cells from primary recipients (*Online Supplementary Figure S4U*). The results demonstrated a significant impairment in the self-renewal capacity of both Alyref$^{+/-}$ and Alyref$^{-/-}$ HSC (*Online Supplementary Figure S4V*). Additionally, both groups exhibited a myeloid-biased potential (*Online Supplementary Figure S4X*), characteristic of aged HSC.

Further exploration of the molecular distinctions among Alyref$^{+/-}$, Alyref$^{-/-}$ and wild-type (WT) HSC, involved RNA-seq analysis of these cells, revealing distinct groupings by principal component analysis (PCA) analysis (*Online Supplementary Figure S4Y*). GSEA unveiled the loss of HSC fingerprint genes and activation of cell aging-related genes in both Alyref$^{-/-}$ and Alyref$^{+/-}$ HSC (*Online Supplementary Figure S4Z*; *Online Supplementary Table S7*).

In summary, these data underscore that targeted dysfunction of *Alyref* recapitulates the characteristics of aged HSC, and demonstrates a dosage-dependent effect.

Dysfunction of RNA transportation impairs hematopoietic stem cells

The aforementioned results strongly suggest a potential role for *Alyref*-mediated RNA transportation in HSC aging. To further investigate this hypothesis, we sought to determine whether the dysfunction of other RNA transporters affects the reconstitution capacity of HSC. To this end, we developed two efficient shRNA targeting *Thoc1* and *Thoc5* (Figure 5A), essential components of the RNA transportation complexes TREX and AREX,[39] respectively. RNA FISH analysis revealed that knockdown of these genes resulted in the accumulation of poly(A)$^+$RNA in the nucleus of hematopoietic stem and progenitor cells (Figure 5B). Subsequently, we conducted competitive transplantation assays to assess the functional impact of their knockdown on HSC. The results demonstrated that knockdown of *Thoc1* and *Thoc5* severely impaired the reconstitution capacity of HSC (Figure 5C, D).

Bulk mRNA nuclear export relies on the RNA export receptor *Nxf1*, which interacts with FG-repeat containing nucleoporins to facilitate RNA translocation.[40,41] We subsequently designed and tested two highly effective shRNA targeting *Nxf1* (*Online Supplementary Figure S5A*). Upon performing the same assay, we observed that *Nxf1* knockdown leads to the accumulation of poly(A)$^+$RNA in the nucleus (Figure 5E) and significantly diminishes the reconstitution capacity of HSC (Figure 5F).

Taken together, these findings demonstrate that dysfunction of RNA transportation genes causes RNA buildup in the nucleus of HSC, thereby compromising their function.

Quantitative refill of *Alyref* rescues the function of aged hematopoietic stem cells by dampening R-Loop and replication stress

We then explored whether overexpression of *Alyref* could rescue the function of aged HSC. To test this hypothesis, we cloned the cDNA of mouse *Alyref* into a lentiviral vector,[42] which resulted in efficient overexpression of ALYREF (*Online Supplementary Figure S6A*). Subsequently, we conducted competitive transplantation assays to assess the functional impact of enforced *Alyref* on HSC. Surprisingly, it was found that overexpression of *Alyref* impaired the reconstitution capacity of aged HSC (Figure 6A). A previous study has indicated that overexpression of *Alyref* leads to the accumulation of RNA in nucleus.[43] To investigate this further, we performed RNA FISH assays to examine the RNA distribution in *Alyref*-overexpressed HSC. The results confirmed that RNA is indeed accumulated in the nucleus upon *Alyref* overexpression (Figure 6B).

The earlier results have demonstrated that *Alyref* modulates the function of HSC in a dosage-dependent manner (*Online Supplementary Figure S4V*). Subsequently, we quantified the protein level of ALYREF in young and aged HSC, revealing a 50% decrease in ALYREF levels in aged HSC (*Online Supplementary Figure S3G, Figure 6C;* left histogram). However, lentiviral-mediated ALYREF overexpression resulted in a 45-fold increase (Figure 6C; right histogram), explaining the cytotoxic effect of *Alyref* overexpression on aged HSC. To precisely replenish ALYREF levels in aged HSC, we developed a quantitative gene expression system (QGES) to compensate for the drop of ALYREF. In this system, QGES-2^{Alyref} exhibits a 2-fold increase (Figure 6D). We conducted competitive transplantation assays to assess the functional role of quantitative refill of ALYREF on aged HSC using QGES-2^{Alyref} system. LSK cells isolated from 18 months old WT mice were infected with QGES-2^{Alyref} and empty control lentivirus. After 72 hours, 4000 CD48$^-$ Sca1$^+$ GFP$^+$ cells were FACS-purified and transplanted into lethally irradiated recipients along with 3×10^5 competitor cells, which were isolated from 2- to 3-month-old CD45.1 mice (*Online Supplementary Figure S6B*). Donor-derived chimerism was examined every 4 weeks until the 16th week. The results showed a mild, though not significant (P=0.18), increase in the QGES-2^{Alyref} group (Figure 6E). Subsequently, we performed secondary transplantation from primary recipients, and the results revealed that aged HSC with quantitative

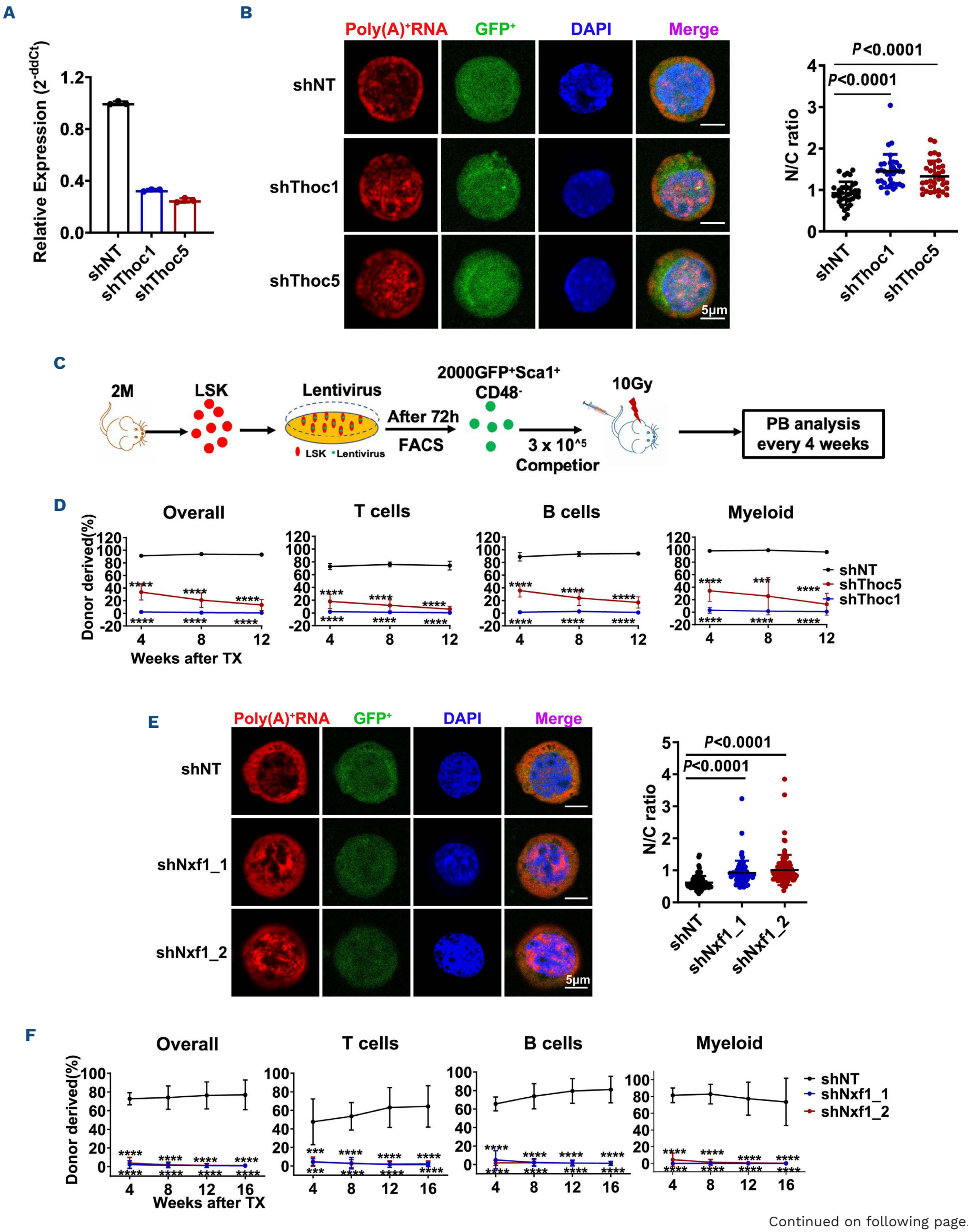

Continued on following page.

Figure 5. Dysfunction of RNA transportation impairs hematopoietic stem cells. (A) Real-time polymerase chain reaction (RT-PCR) analysis of the knockdown efficiency of small hairpin (sh)RNA against *Thoc1* and *Thoc5* using freshly isolated LSK cells. (B, left representative image) Representative images depicting the distribution of poly(A)$^+$RNA in shNT, shThoc1 and shThoc5 hemtopoietic stem and progenitor cells (HSPC). Freshly isolated LSK cells from young mice (2 months) were infected with lentivirus carrying *Thoc1* shRNA, *Thoc5* shRNA or control shRNA. After 3 days, GFP$^+$ cells were purified for Poly(A)$^+$RNA fluorescence *in situ* hybridization (FISH). The panels are shown at the same exposure. Poly(A)$^+$RNA was detected using a Cy3-labeled oligo(dT)$_{50}$ probe. The cell nuclei were stained with DAPI. (B, right dot plot) The dot plots show the ratio of nuclear to cytoplasmic poly(A)$^+$RNA signals ratio in shNT, shThoc1 and shThoc5 HSPC. Data are presented as mean ± standard deviation (SD). N and C indicate nuclear and cytoplasmic FISH signals, respectively. N/C ratios were determined for at least 33 cells in each experiment. (C) Experimental design of the competitive transplantation assay. Freshly isolated LSK cells from young mice (2 months old) were infected by lentivirus carrying *Thoc1* shRNA, *Thoc5* shRNA or control shRNA, labeled by GFP fluorescence. Three days later, 2000 GFP$^+$Sca1$^+$CD48$^-$ cells were purified and transplanted into lethally irradiated recipients (CD45.2) along with 3×10^5 competitor cells (CD45.1). Chimerism in peripheral blood was evaluated every 4 weeks until the 12th week. (D) These line plots depict the percentage of donor-derived cells (overall, B cells, T cells, myeloid cells) in the peripheral blood of recipients. N=4-7 recipients per group, data are presented as mean ± SD. (E, left representative image) Representative images depicting the distribution of Poly(A)$^+$RNA in both shNT and shNxf1 HSPC. Freshly isolated LSK cells from young mice (2 months old) were infected with lentivirus carrying *Nxf1* shRNA or control shRNA. After 3 days, GFP$^+$ cells were purified for Poly(A)$^+$RNA FISH. The panels are shown at the same exposure. Poly(A)$^+$RNA was detected using a Cy3-labeled oligo(dT)$_{50}$ probe. The cell nuclei were stained with DAPI. (E, right dot plot) The dot plot shows the ratio of nuclear to cytoplasmic poly(A)$^+$RNA signals ratio in shNT and shNxf1 HSPC. Data are presented as mean ± SD. N and C indicate nuclear and cytoplasmic FISH signals, respectively. N/C ratios were determined for at least 78 cells in each experiment. (F) These line plots depict the percentage of donor-derived cells (overall, B cells, T cells, myeloid cells) in the peripheral blood of recipients. N=6-7 recipients per group, data are shown as mean ± SD.

expression of *Alyref* significantly outcompeted the control group (Figure 6E), indicating that precise compensation of ALYREF in aged HSC significantly rescues their self-renewal capacity.

By conducting RNA FISH, we observed that the aberrant RNA accumulation in the nucleus of aged HSC is rescued by precise refill of ALYREF (Figure 6F). Moreover, we observed dramatic reduction in R-Loop (*Online Supplementary Figure S6C, D*), γH2AX (*Online Supplementary Figure S6E, F*) and RPA (*Online Supplementary Figure S6G, H*) foci in HSC carrying the QGES-2^{Alyref}- construct. The replication fork assay showed a decrease in replication stress in the QGES-2^{Alyref} group (*Online Supplementary Figure S6I, J*).

Collectively, these data indicate that precise refill of ALYREF in aged HSC rescues the self-renewal capacity of aged HSC by diminishing DNA damage and replication stress.

Discussion

Our study demonstrates that the imbalance of RNA distribution between the nucleus and cytoplasm, mediated by compromised RNA transportation, contributes to HSC aging by inducing R-Loops and subsequent replication stress (*Online Supplementary Figure S6K*). Furthermore, quantitative refill of ALYREF ameliorates the function of aged HSC. This study delves into the functional role of R-Loop in HSC aging and unveils a novel mechanism driving HSC aging.

RNA imbalance promotes hematopoietic stem cell aging

The homeostasis of RNA distribution between nucleus and cytoplasm is vital for cellular function, wherein RNA transportation playing a central role. In this study, we observed that the RNA distribution between the nucleus and cytoplasm of aged HSC became unbalanced, stemming from the decline of *Alyref*. Targeted dysfunction of *Alyref* recapitulated the phenotype of aged HSC, while precise refill of it rejuvenated the function of aged HSC by restoring RNA shuttling and dampening R-Loops. Since stable expression of *Alyref* is crucial for hematopoietic homeostasis and HSC function, investigating the molecular mechanisms compromising *Alyref* during aging is worthy of further study. A previous study has reported that *Alyref* specifically interacts with m^{5}C RNA.[44] It is intriguing to explore the specificity of RNA transported by *Alyref*, whether it is mediated by m^{5}C or other RNA modifications.

DNA damage *versus* aging and aging-related diseases

Aging is the highest risk factor for many diseases. It has been reported that aged blood induces cell and tissue senescence and *vice versa*, young blood revitalizes aged organism.[45-49] Aged HSC compromise the function of blood system. Therefore, rejuvenating aged HSC will benefit the function of aged organism.

On the basis of R-Loop findings of this study, we open a new aspect in the aging study. Firstly, we demonstrated that aging-accumulated R-loop is the resource of replication stress. Accumulated R-Loop results in more displaced ssDNA, which is vulnerable to damage.[20] In addition, accumulated R-Loop interfere with proper DNA repair machinery, especially the homologous recombination pathway. Secondly, R-Loop is a multi-faced player in modulating transcription by influencing promoter activity or chromatin structure, altering the local chromatin environment, promoting epigenetic modifications like DNA methylation or histone modifications.[20] Hence, in addition to R-Loop-induced replication stress, whether other aforementioned molecular events, such as those involving long non-coding RNA and DNA damage response RNA,[50] participate in regulating hematopoietic stem cell aging is worthy of further exploration.

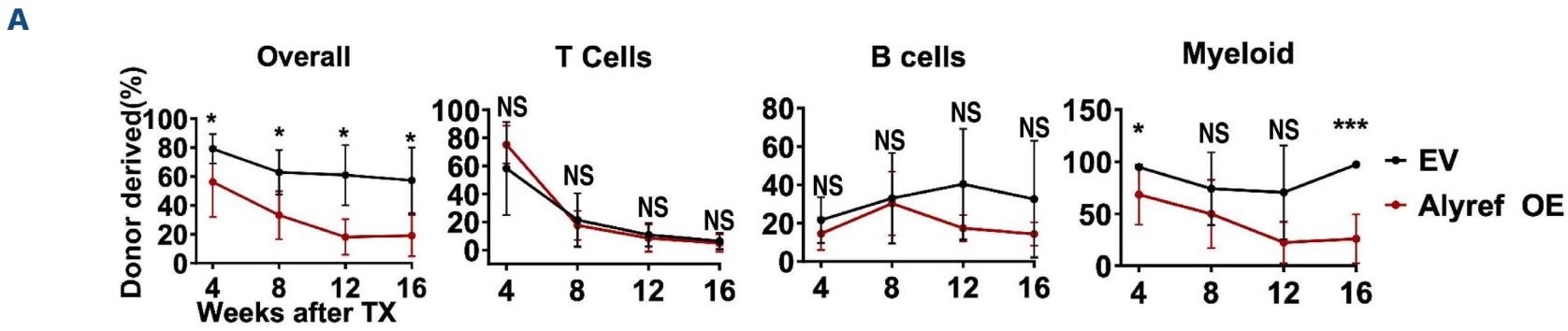

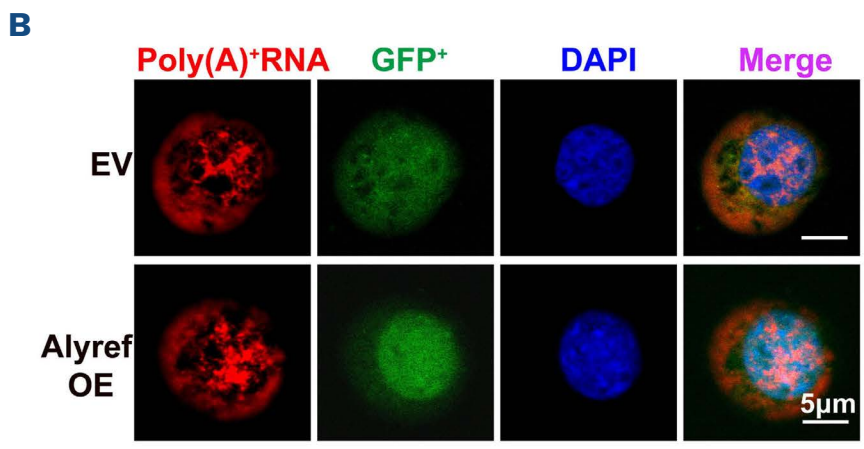

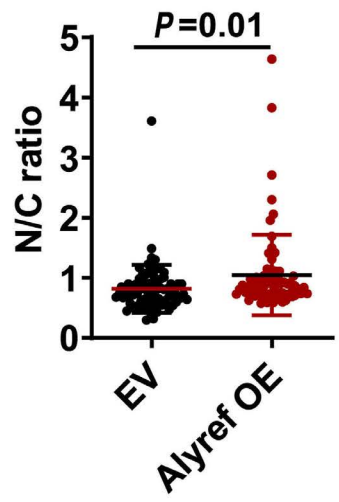

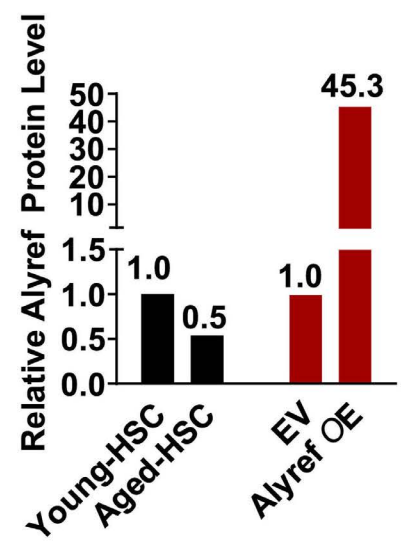

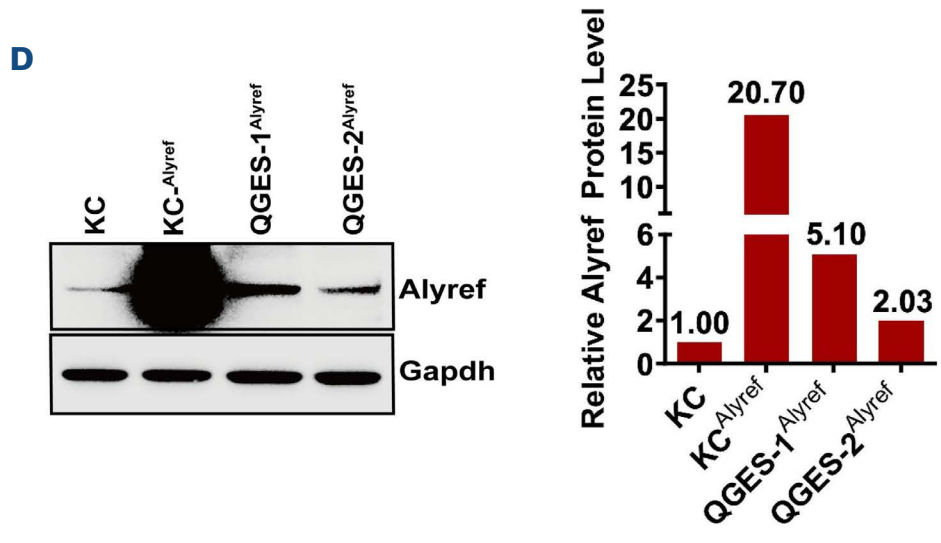

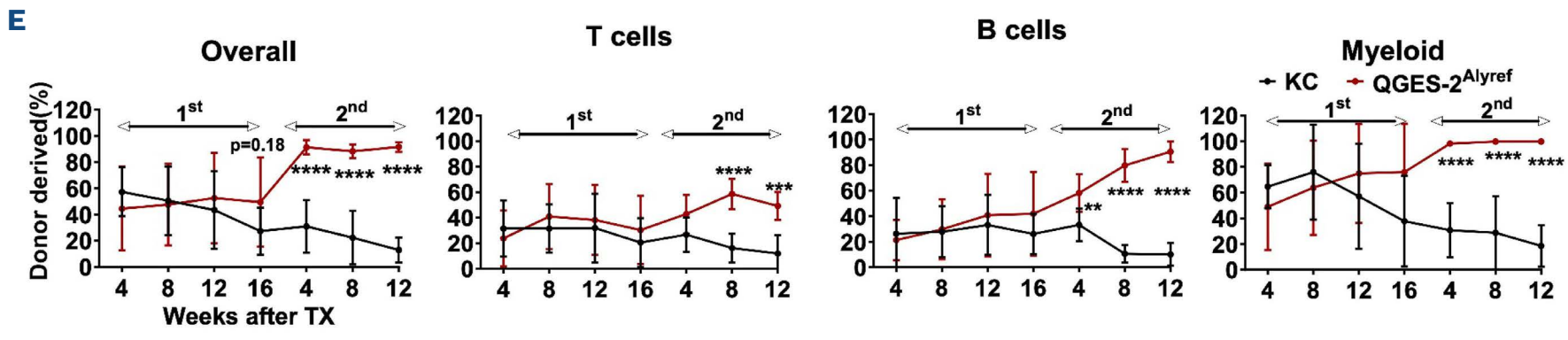

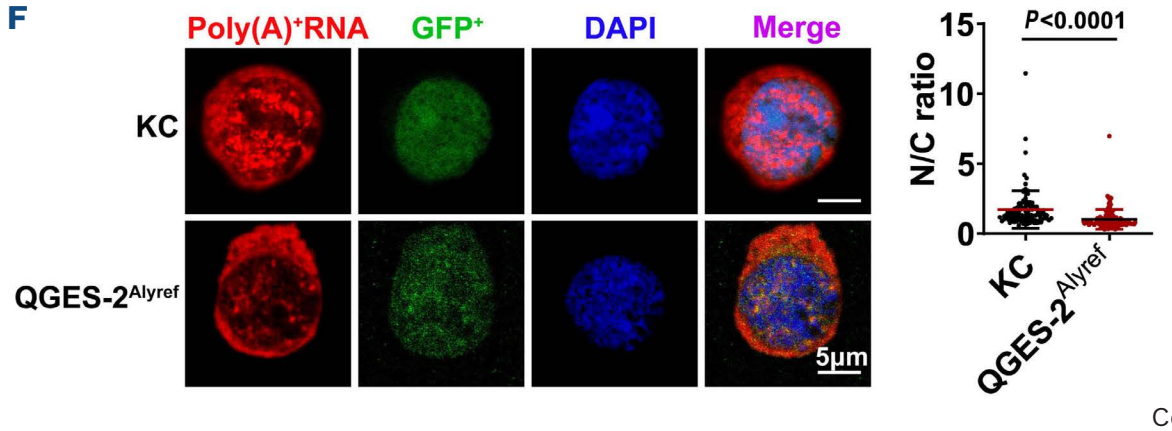

Continued on following page.

Figure 6. Quantitative refill of *Alyref* rescues the function of aged hematopoietic stem cells by dampening R-Loop and replication stress. (A) Line plots depicting the proportion of donor-derived cells (overall, T cells, B cells, myeloid cells) in the peripheral blood of recipients. N=5-7 recipients per group. Data are represented as mean ± standard deviation (SD). (B, left representative image) Representative images depicting the distribution of Poly(A)$^+$RNA in empty vector (EV) and *Alyref* overexpressed (OE) hematopoietic stem cells (HSC). The panels are shown at the same exposure. Poly(A)$^+$RNA was detected using a Cy3-labeled oligo(dT)$_{50}$ probe. The cell nuclei were stained with DAPI. (B, right dot plot) Dot plots depicting the nuclear and cytoplasmic (N/C) poly(A)$^+$RNA signals ratio in both EV and *Alyref* OE HSC. Data are represented as mean ± SD. N and C indicate nuclear and cytoplasmic fluorescence *in situ* hybridization (FISH) signals, respectively. N/C ratios were determined for a minimum of 73 cells in each experiment. (C) Histograms illustrate the quantitative analysis of ALYREF protein levels in young/aged HSC and EV/*Alyref* OE HSPC. Data were analyzed using image J. (D, left representative western blot) Representative western blot showing the expression of ALYREF. NIH-3T3 cells were infected with QGES-^{1Alyref}, QGES-2^{Alyref}, KC^{Alyref} and control lentivirus (KC). After 3 days, GFP$^+$ cells were purified for western blot. (D, right histogram) Histograms depicting the quantitative ALYREF protein in QGES-1^{Alyref}, QGES-2^{Alyref}, KC^{Alyref} and KC (Figure 6D, left representative western blot). Data were analyzed using image J. (E) Line plots depicting the proportion of donor-derived cells (overall, B cells, T cells, myeloid cells) in the peripheral blood of recipients. N=6-7 recipients per group. Data are represented as mean ± SD. (F, left representative image) Representative images depicting the distribution of Poly(A)$^+$RNA in QGES-2^{Alyref} and KC HSPC using freshly isolated GFP$^+$ LSK cells from the recipients of (*Online Supplementary Figure S6B*) at the end of the 16th week after transplantation. The panels are shown at the same exposure. Poly(A)$^+$RNA was detected using a Cy3-labeled oligo(dT)$_{50}$ probe. The cell nuclei were stained with DAPI. (F, right dot plot) Dot plots depicting the nuclear and cytoplasmic poly(A)$^+$RNA signals ratio in KC and QGES-2^{Alyref} HSPC. Data are represented as mean ± SD. N and C indicate nuclear and cytoplasmic FISH signals, respectively. N/C ratios were determined for a minimum of 108 cells in each experiment.

Disclosures

No conflicts of interest to disclose.

Contributions

Conceptualization by JW. Methodology by RC, QD and LZ. Investigation by RC, QD, LZ, HH, YD, QS, TS, TC and JW. Formal analysis by JW. Resources by JW. Writing by TC and JW. Funding acquisition by QD and JW. Supervision by TC and JW.

Acknowledgments

We thank Dr. Hong Cheng (Institute of Biochemistry and Cell Biology, University of Chinese Academy of Sciences) for providing constructive suggestions for this project.

Funding

This work was supported by grant numbers 2024-I2M-ZD-010, W2441024, 82250002 and 92249305 (to JW) from CAMS Innovation Fund for Medical Sciences (CIFMS) and the National Natural Science Foundation of China; and by 62103397 (to QD) from National Natural Scientific Foundation of China.

Data-sharing statement

For original data, please contact the corresponding author JW. RNA-seq, cytoplasmic and nuclear RNA-seq, ss-DRIP-seq data are available at GEO under accession number GSE239301. Whole genome sequencing data is available at SRA under accession number PRJNA1000120.

References

1. Brunet A, Goodell MA, Rando TA. Ageing and rejuvenation of tissue stem cells and their niches. Nat Rev Mol Cell Biol. 2023;24(1):45-62.
2. Jayarajan J, Milsom MD. The role of the stem cell epigenome in normal aging and rejuvenative therapy. Hum Mol Genet. 2020;29(R2):R236-R247.
3. Tümpel S, Rudolph KL. Quiescence: good and bad of stem cell aging. Trends Cell Biol. 2019;29(8):672-685.
4. Haas S, Trumpp A, Milsom MD. Causes and consequences of hematopoietic stem cell heterogeneity. Cell Stem Cell. 2018;22(5):627-638.
5. Mejia-Ramirez E, Florian MC. Understanding intrinsic hematopoietic stem cell aging. Haematologica. 2020;105(1):22-37.
6. Geiger H, de Haan G, Florian MC. The ageing haematopoietic stem cell compartment. Nat Rev Immunol. 2013;13(5):376-389.
7. Geiger H, Rudolph KL. Aging in the lympho-hematopoietic stem cell compartment. Trends Immunol. 2009;30(7):360-365.
8. DeGregori J. Aging, inflammation, and HSC. Blood. 2020;136(2):153-154.
9. Jamieson CHM, Weissman IL. Stem-cell aging and pathways to precancer evolution. N Engl J Med. 2023;389(14):1310-1319.
10. Flach J, Bakker ST, Mohrin M, et al. Replication stress is a potent driver of functional decline in ageing haematopoietic stem cells. Nature. 2014;512(7513):198-202.
11. Rossi DJ, Bryder D, Seita J, Nussenzweig A, Hoeijmakers J, Weissman IL. Deficiencies in DNA damage repair limit the function of haematopoietic stem cells with age. Nature. 2007;447(7145):725-729.
12. Schumacher B, Pothof J, Vijg J, Hoeijmakers JH. The central role of DNA damage in the ageing process. Nature. 2021;592(7856):695-703.
13. Wang J, Sun Q, Morita Y, et al. A differentiation checkpoint limits hematopoietic stem cell self-renewal in response to DNA damage. Cell. 2012;148(5):1001-1014.
14. He H, Wang Y, Tang B, et al. Aging-induced MCPH1 translocation activates necroptosis and impairs hematopoietic stem cell function. Nat Aging. 2024;4(4):510-526.
15. He H, Wang Y, Zhang X, et al. Age-related noncanonical TRMT6-TRMT61A signaling impairs hematopoietic stem cells.

Nat Aging. 2024;4(2):213-230.
16. Gaillard H, García-Muse T, Aguilera A. Replication stress and cancer. Nat Rev Cancer. 2015;15(5):276-289.
17. Saxena S, Zou L. Hallmarks of DNA replication stress. Mol Cell. 2022;82(12):2298-2314.
18. Zeman MK, Cimprich KA. Causes and consequences of replication stress. Nat Cell Biol. 2013;16(1):2-9.
19. Petermann E, Lan L, Zou L. Sources, resolution and physiological relevance of R-loops and RNA-DNA hybrids. Nat Rev Mol Cell Biol. 2022;23(8):521-540.
20. Hegazy YA, Fernando CM, Tran EJ. The balancing act of R-loop biology: the good, the bad, and the ugly. J Biol Chem. 2000;295(4):905-913.
21. Xu W, Xu H, Li K, et al. The R-loop is a common chromatin feature of the Arabidopsis genome. Nat Plants. 2017;3(9):704-714.
22. Li Y, Song Y, Xu W, et al. R-loops coordinate with SOX2 in regulating reprogramming to pluripotency. Sci Adv. 2020;6(24):eaba0777.
23. Boguslawski SJ, Smith DE, Michalak MA, et al. Characterization of monoclonal antibody to DNA.RNA and its application to immunodetection of hybrids. J Immunol Methods. 1986;89(1):123-130.
24. Chang EY, Tsai S, Aristizabal MJ, et al. MRE11-RAD50-NBS1 promotes Fanconi anemia R-loop suppression at transcription-replication conflicts. Nat Commun. 2019;10(1):4265.
25. Hartono SR, Malapert A, Legros P, Bernard P, Chédin F, Vanoosthuyse V. The affinity of the S9.6 antibody for double-stranded RNAs impacts the accurate mapping of R-Loops in fission yeast. J Mol Biol. 2018;430(3):272-284.
26. Jauregui-Lozano J, Escobedo S, Easton A, Lanman NA, Weake VM, Hall H. Proper control of R-loop homeostasis is required for maintenance of gene expression and neuronal function during aging. Aging Cell. 2022;21(2):e13554.
27. Buisson R, Boisvert JL, Benes CH, Zou L. Distinct but concerted roles of ATR, DNA-PK, and Chk1 in countering replication stress during SPhase. Mol Cell. 2015;1011-1024.
28. Toledo LI, Altmeyer M, Rask MB, et al. ATR prohibits replication catastrophe by preventing global exhaustion of RPA. Cell. 2013;155(5):1088-1103.
29. Tsai JJ. The transcription factor nuclear factor erythroid-2 related 2 regulates hematopoietic stem cell function and T-cell alloreactivity. https://ecommons.cornell.edu/items/61d5867b-7b82-444b-bb55-a1f4f6ffcc0e. Accessed July 17, 2023.
30. Nguyen HD, Yadav T, Giri S, Saez B, Graubert TA, Zou L. Functions of replication protein A as a sensor of R loops and a regulator of RNaseH1. Mol Cell. 2017;65(5):832-847.e4.
31. Rychlik MP, Chon H, Cerritelli SM, Klimek P, Crouch RJ, Nowotny M. Crystal structures of RNase H2 in complex with nucleic acid reveal the mechanism of RNA-DNA junction recognition and cleavage. Mol Cell. 2010;40(4):658-670.
32. Kabeche L, Nguyen HD, Buisson R, Zou L. A mitosis-specific and R loop-driven ATR pathway promotes faithful chromosome segregation. Science. 2018;359(6371):108-114.
33. Chen Y, Fang S, Ding Q, et al. ADGRG1 enriches for functional human hematopoietic stem cells following ex vivo expansion-induced mitochondrial oxidative stress. J Clin Invest. 2021;131(20):e148329.
34. Kirschner K, Chandra T, Kiselev V, et al. Proliferation drives aging-related functional decline in a subpopulation of the hematopoietic stem cell compartment. Cell Rep. 2017;19(8):1503-1511.
35. Sun D, Luo M, Jeong M, et al. Epigenomic profiling of young and aged HSCs reveals concerted changes during aging that reinforce self-renewal. Cell Stem Cell. 2014;14(5):673-688.
36. Maryanovich M, Zahalka AH, Pierce H, et al. Adrenergic nerve degeneration in bone marrow drives aging of the hematopoietic stem cell niche. Nat Med. 2018;24(6):782-791.
37. Grover A, Sanjuan-Pla A, Thongjuea S, et al. Single-cell RNA sequencing reveals molecular and functional platelet bias of aged haematopoietic stem cells. Nat Commun. 2016;7:11075.
38. Renders S, Svendsen AF, Panten J, et al. Niche derived netrin-1 regulates hematopoietic stem cell dormancy via its receptor neogenin-1. Nat Commun. 2021;12(1):608.
39. Reed R, Cheng H. TREX, SR proteins and export of mRNA. Curr Opin Cell Biol. 2005;17(3):269-273.
40. Viphakone N, Hautbergue GM, Walsh M, et al. TREX exposes the RNA-binding domain of Nxf1 to enable mRNA export. Nat Commun. 2012;3:1006.
41. Fribourg S, Braun IC, Izaurralde E, Conti E. Structural basis for the recognition of a nucleoporin FG repeat by the NTF2-like domain of the TAP/p15 mRNA nuclear export factor. Mol Cell. 2001;8(3):645-656.
42. He H, Xu P, Zhang X, et al. Aging-induced IL27Ra signaling impairs hematopoietic stem cells. Blood. 2020;136(2):183-198.
43. Hautbergue GM, Hung ML, Walsh MJ, et al. UIF, a New mRNA export adaptor that works together with REF/ALY, requires FACT for recruitment to mRNA. Curr Biol. 2009;19(22):1918-1924.
44. Yang X, Yang Y, Sun BF, et al. 5-methylcytosine promotes mRNA export - NSUN2 as the methyltransferase and ALYREF as an m(5)C reader. Cell Res. 2017;27(5):606-625.
45. Ma S, Wang S, Ye Y, et al. Heterochronic parabiosis induces stem cell revitalization and systemic rejuvenation across aged tissues. Cell Stem Cell. 2022;29(6):990-1005.e10.
46. Jeon O, Mehdipour M, Gil TH, et al. Systemic induction of senescence in young mice after single heterochronic blood exchange. Nat Metab. 2022;4(8):995-1006.
47. Zhang B, Lee DE, Trapp A, et al. Multi-omic rejuvenation and lifespan extension on exposure to youthful circulation. Nat Aging. 2023;3(8):948-964.
48. Yousefzadeh MJ, Flores RR, Zhu Y, et al. An aged immune system drives senescence and ageing of solid organs. Nature. 2021;594(7861):100-105.
49. Ross JB, Myers LM, Noh JJ, et al. Depleting myeloid-biased haematopoietic stem cells rejuvenates aged immunity. Nature. 2024;628(8006):162-170.
50. Michelini F, Pitchiaya S, Vitelli V, et al. Damage-induced lncRNAs control the DNA damage response through interaction with DDRNAs at individual double-strand breaks. Nat Cell Biol. 2017;19(12):1400-1411.